BBC RD 1985/9

RESEARCH DEPARTMENT

REPORT

DIGITAL TELEVISION ROUTING SYSTEMS:
An introduction to integrated optical waveguide techniques and devices

J.P. Willson, B.Sc., Ph.D., A.R.C.S., D.I.C.

Research Department, Engineering Division
THE BRITISH BROADCASTING CORPORATION

August, 1985

BBC RD 1985/ 9

DIGITAL TELEVISION ROUTING SYSTEMS: AN INTRODUCTION TO INTEGRATED OPTICAL WAVEGUIDE TECHNIQUES AND DEVICES

J.P. Willson, B.Sc., Ph.D., A.R.C.S., D.I.C.

Summary

The development of a digital standard for the coding of component video signals has raised the problem of the appropriate technology to be used for the routing and distribution of such signals within a television studio centre. Optical fibres offer a number of advantages over coaxial cable, such as high bandwidth, low loss, and small size. However, a major problem with optical transmission is that of routing the optical signals. One possible solution is to use integrated optical switches. This Report considers the application of such devices for fabricating a large (100 x 100) array suitable for an all-digital BBC Television Centre. The main conclusion is that there remains a great deal of development to be done before such an array is feasible.

Issued under the Authority of

M.E.B. Moffat

Head of Research Department

Research Department, Engineering Division,
BRITISH BROADCASTING CORPORATION

August 1985
(EL-174)

This Report may not be reproduced in any form without the written permission of the British Broadcasting Corporation.

It uses SI units in accordance with B.S. document PD 5686.

DIGITAL TELEVISION ROUTING SYSTEMS: AN INTRODUCTION TO INTEGRATED OPTICAL WAVEGUIDE TECHNIQUES AND DEVICES

J.P. Willson, B.Sc., Ph.D., A.R.C.S., D.I.C.

Section Title Page

Summary .... Title Page

1. Introduction 1

2. An introduction to the theory of optical waveguides 1

2.1. Planar waveguides 1
2.2. Stripe waveguides 4

3. Materials and fabrication techniques 5

3.1. Glass waveguides 5
3.2. Lithium niobate ($LiNbO_3$) waveguides 5
3.2.1. *Titanium indiffusion in lithium niobate* 5
3.2.2. Proton exchange in lithium niobate 6
3.3. Semiconductor waveguides 6

4. Switches 7

4.1. Definition of extinction ratio 7
4.2. The X-type or cross-over switch 8
4.3. The directional coupler switch 9

5. Switch arrays 11

5.1. Blocking arrays 11
5.1.1. Blocking arrays using directional coupler elements 12
5.1.2. Blocking arrays using X-type switch elements 12
5.2. Non-blocking switch arrays 12
5.2.1. X-type switch elements in non-blocking, partial-tap arrays 14

6. Modulators and other devices 15

6.1. The phase modulator 15
6.2. The Mach-Zehnder interferometer (intensity and frequency modulator) 15
6.3. Polarisation controllers 16
6.4. Waveguide optical bandpass filters 16

7. Conclusions 17

8. References 18

9. Appendices 21

9.1. Appendix 1: Photolithographic techniques 21

9.2. Appendix 2: Definition of extinction ratio 21

9.3. Appendix 3: Calculation of signal-to-noise ratio in a partial-tap non-blocking array using X-type switch elements 23

9.4. Appendix 4: List of Symbols 24

© BBC 2006. All rights reserved. Except as provided below, no part of this document may be reproduced in any material form (including photocopying or storing it in any medium by electronic means) without the prior written permission of BBC Research & Development except in accordance with the provisions of the (UK) Copyright, Designs and Patents Act 1988.

The BBC grants permission to individuals and organisations to make copies of the entire document (including this copyright notice) for their own internal use. No copies of this document may be published, distributed or made available to third parties whether by paper, electronic or other means without the BBC's prior written permission. Where necessary, third parties should be directed to the relevant page on BBC's website at http://www.bbc.co.uk/rd/pubs/ for a copy of this document.

DIGITAL TELEVISION ROUTING SYSTEMS: AN INTRODUCTION TO INTEGRATED OPTICAL WAVEGUIDE TECHNIQUES AND DEVICES

J.P. Willson, B.Sc., Ph.D., A.R.C.S., D.I.C.

1. Introduction

The development of a standard for the digital coding of component video signals[1] has raised the problem of the appropriate technology to be used for the distribution of such signals within a studio centre. There is a wide range of possible methods, such as serial or parallel format, coaxial or optical links, and electronic or optical switching. The different methods are briefly described elsewhere[2], and a series of Reports is in preparation describing some of the options in more detail. The aim of this Report is to introduce the basic ideas of integrated optics in their application to optical switching.

Optical fibres possess a number of attractive properties for the transmission of data, such as large bandwidth, low loss, and small dimensions[3]. However, a major problem is the routing of optical signals. One possible solution is to use conventional optics such as mirrors and lenses in a mechanical system[4]. Although this technology is well established, there are some doubts about its suitability in an operational system. Alternatively, the routing might be performed by integrated optical switches[5].

Integrated optics is the study of the propagation of light in dielectric waveguides and waveguide devices. In essence, it can be considered as the study of optical integrated circuits. The major advantage of integrated optics is that it allows the manipulation of optical signals without the need for an intermediate electronic stage. Furthermore, because the dimensions involved are small (typically μm), and the optical and electric fields have a high degree of overlap, the voltages required for manipulation are low. Typically, the operating voltages of integrated optical devices are several orders of magnitude lower than is the case for conventional optics. Consequently, integrated optics offers the possibility of high speed (>10Gbits/s), low power (~mW)[5] optical signal manipulation.

A wide variety of devices has been developed, including routing switches, modulators, polarisation controllers, and tunable bandpass filters[5]. In fact, the integrated optical equivalents of most conventional optical devices have been demonstrated, as well as some devices that cannot be made conventionally.

This Report outlines the basic principles of optical waveguides, and describes the more common waveguide materials and fabrication techniques. In addition, a number of devices which are potentially useful in optical fibre communication systems are described.

2. An introduction to the theory of optical waveguides

In the most general sense, integrated optics encompasses both optical integrated circuits, and optical fibre communication systems. However, because of the broad scope of both of these fields, they are generally considered separately. Consequently, the term integrated optics is now only applied to optical integrated circuits, which is the area covered in this Report.

2.1. Planar waveguides

The simplest waveguide is the planar structure shown in Fig.1, where a guiding layer, or film, of thickness h is sandwiched between cover and substrate layers. The light is only confined in the x direction, with the dimensions of the guide in the y and z directions assumed to be infinite. For waveguiding to occur, the refractive index of the film (n_f) has to be greater than that of the cover

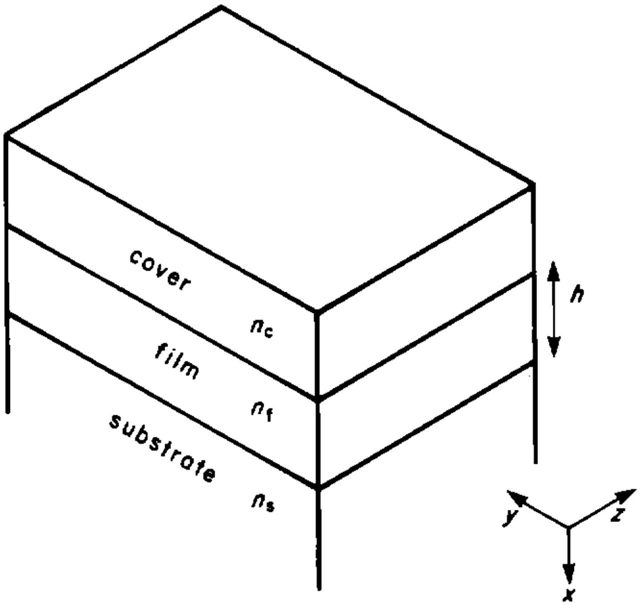

Fig. 1 – A schematic diagram of a planar waveguide.

(n_c) and substrate (n_s). Usually the refractive index of the cover layer is less than that of the substrate, in which case the structure is referred to as an asymmetric planar waveguide. The asymmetric case is discussed below.

The theory of the propagation of light in planar optical waveguides has been extensively studied (see the review in Reference 5). However, a useful, simple, physical model of propagation is the "ray-optics" approach. In this model, the light is considered as a set of plane waves. The plane waves are then described by a set of rays, which are normal to the wavefronts.

Light launched into the film is guided by total internal reflection (TIR) at the film/cover and film/substrate interfaces. The light can therefore be pictured as rays zig-zagging along the waveguide as shown in Fig. 2. However, the angle of incidence, θ, of the light rays must be greater than the critical angle of the interface for TIR to occur. Therefore the ray angle θ is limited to a minimum value, determined by the refractive indices. (Note that θ is measured with respect to the normal to the interface).

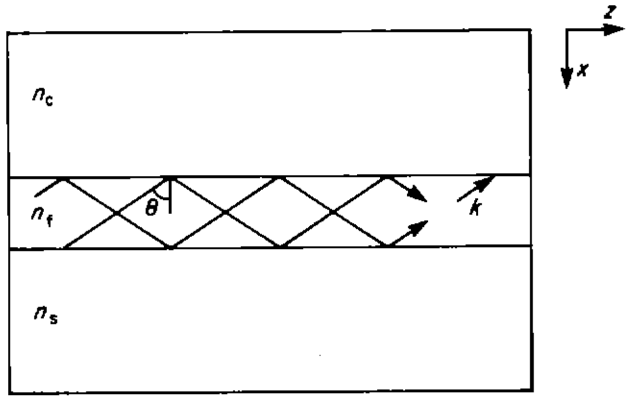

Fig. 2 — The ray-optics representation of a mode of a planar waveguide.

Furthermore, the total phase-shift of the wavefront as it travels from one interface to the other and back again (including the phase-shifts due to reflection at the interfaces) must be a multiple of 2π to give constructive interference. This means that within the range of angles where TIR occurs, only certain angles are allowed. These angles correspond to the modes of the guide.

Each mode is described by a wavevector K, which has a magnitude k_f given by:

$$k_f = kn_f \tag{1}$$

where k is the magnitude of the wavevector in free space ($k = 2\pi/\lambda$). The z-component of the wavevector in the plane of the guide is called the propagation constant of the mode, β, and is given by:

$$\beta = kn_f \sin\theta \tag{2}$$

For guided modes, β has to lie in the range:

$$kn_s \leqslant \beta \leqslant kn_f \tag{3}$$

For $\beta < kn_s$, the light is not totally reflected at the interface, and radiates into the substrate.

The limits defined by Equation 3 can be more easily visualised by defining an "effective guide refractive index" N by:

$$N = \beta_{/k} \tag{4}$$

For guided modes, Equation 3 shows that N lies in the range:

$$n_s \leqslant N \leqslant n_f \tag{5}$$

Although it is now possible to describe the properties of particular waveguides in terms of, for example, the mode effective indices, and film thickness, the description does not provide much insight for relating waveguides of different materials and structures. More useful parameters are the normalised frequency, V, and the normalised guide index, b.

The normalised frequency is defined as:

$$V = kb(2n_s\Delta)^{\frac{1}{2}} = \frac{2\pi b(2n_s\Delta)^{\frac{1}{2}}}{\lambda} \tag{6}$$

where $\Delta = (n_f - n_s)$ is the refractive index difference between the film and substrate. The normalised guide index, b, is defined as:

$$b = (N^2 - n_s^2)/(n_f^2 - n_s^2) \tag{7}$$

These two parameters can then be used to describe the modal propagation characteristics of planar waveguides. However, the modal characteristics also depend on the polarisation of the light because the phase-shift of the wavefronts due to reflection at the interfaces is a function of polarisation. We can therefore define two sets of modes. If the electric component of the optical field is parallel to the plane of the guide, the modes are referred to as transverse electric or TE. If the magnetic component is parallel to the plane of the guide, the modes are transverse magnetic or TM. The different propagation characteristics of the two sets of modes can be described in terms of the guide asymmetry, defined as:

$$a_{TE} = (n_s^2 - n_c^2)/(n_f^2 - n_s^2) \qquad (8)$$

for TE modes, and by:

$$a_{TM} = (n_f^4/n_c^4)\ (n_s^2 - n_c^2)/(n_f^2 - n_s^2) \qquad (9)$$

for the TM modes. The asymmetry parameters range from zero for perfect symmetry ($n_s = n_c$) to infinity for strong asymmetry ($n_s \neq n_c$ and $n_s \approx n_f$). The asymmetry is constant for a given substrate/cover/film combination.

The normalised frequency and guide index, and the measure of asymmetry can be used to calculate a set of general dispersion curves for planar waveguides. Fig. 3 shows the dispersion curves for a step refractive index planar waveguide, with the modes designated by a label m^6. For each value of m, curves are drawn for several values of asymmetry. If the V value and asymmetry of a guide is known, the number of modes, and their propagation constants can be determined. For example, if $V = 6.0$, and the asymmetry $a_{TE} = 10$, then the guide will suppport two TE modes with $b = 0.3$ and $b = 0.81$. The number of modes can be controlled by varying, for example, the index difference Δ, or the film thickness, h (Equation 6).

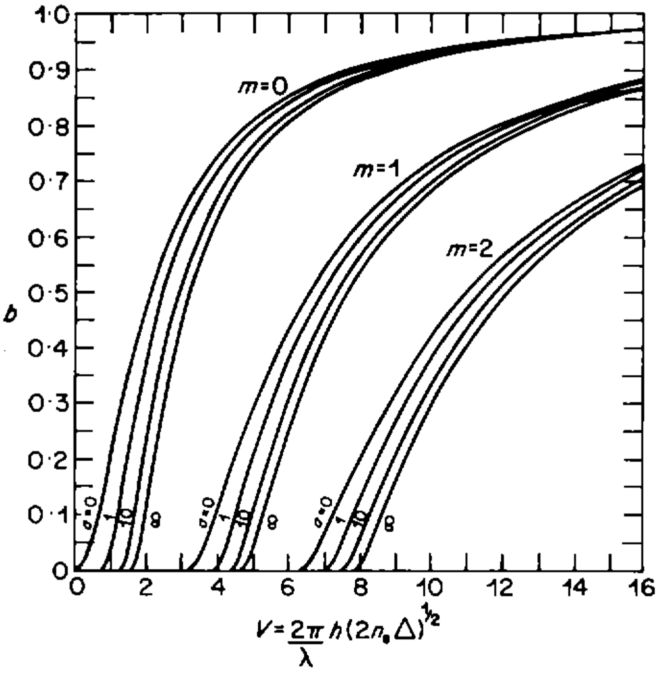

Fig. 3 – The dispersion curves for a step refractive-index-profile planar waveguide (after Reference 6).

It should be noted that Fig. 3 is valid only for an ideal step refractive index profile. Similar sets of curves have been calculated for other index profiles such as the Gaussian, which correspond more closely to experimental devices fabricated by diffusion processes[7].

More rigorous analyses of the properties of dielectric waveguides show that each mode has a different optical field distribution[5]. In fact, the modes can be pictured as corresponding to transverse standing wave patterns in the guide. For example, the three lowest order TE modes corresponding to m=0 to 2 are shown in Fig. 4. A useful rule of thumb is that there are m zeroes in the field distribution for each mode. In addition, it should be noted that the optical field is not completely confined to a high-index layer as in the simple ray optics model, but has exponential tails which extend into the substrate and cover layers. It is the existence of these tails of the field which gives rise to the coupling effects utilised in some of the waveguide switches described in later Sections.

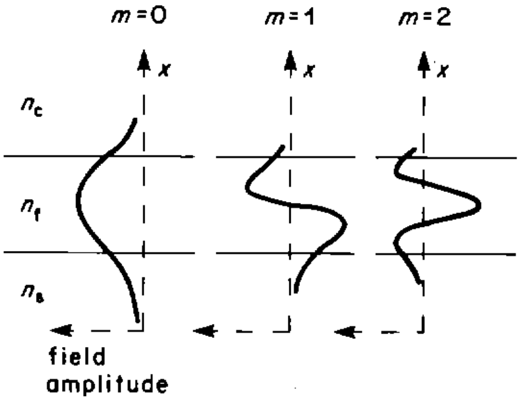

Fig. 4 – The optical field distributions of the three lowest-order modes of an asymmetric planar waveguide.

Theoretically, dielectric waveguides are lossless. However, in practice defects and inhomogeneities cause a finite loss due to scattering[8]. The value of the loss is strongly dependent on substrate material and fabrication method. Experimental results will be given in Section 3.

An inherent disadvantage of planar waveguides is the lack of confinement in the transverse, y, direction. In many cases, such confinement is required. For example, control voltages can be reduced by improving the overlap between optical and electrical fields. Furthermore, some optical processing requires that the optical signal be directed around the substrate to different devices, which is most easily achieved by using stripe (or channel) waveguides.

2.2. Stripe waveguides

The additional confinement required for stripe waveguides can be provided by a number of different structures, four of which are shown in Fig. 5. In all cases, the guided light is primarily confined to the material with index n_f, and width W.

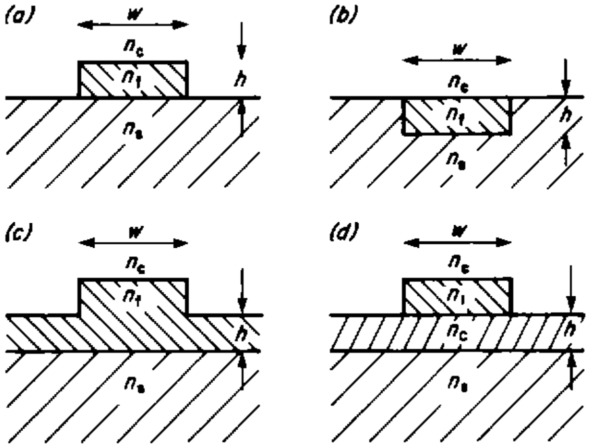

Fig. 5 — Types of stripe waveguide:

a) a raised stripe guide
b) an embedded stripe guide
c) a ridge or rib guide
d) a strip-loaded guide

Fig. 5(a) shows a raised stripe guide which can be fabricated by starting with a planar guide, masking the stripe and removing the unwanted material sputtering or etching. Fig. 5(b) is an embedded guide which is the type of profile produced by ion diffusion techniques, such as titanium diffusion in lithium niobate (Section 3.2.1). Fig. 5(c) is a ridge or rib guide which is essentially a raised stripe guide with only partial removal of the surrounding planar guide. The final example (Fig. 5(d)) is a strip-loaded guide where a stripe of material of lower index $n_l < n_f$ is deposited on to a planar guide. The latter two types are reported to require less critical fabrication techniques, and are commonly used for semiconductor (e.g. gallium arsenide) waveguides.

The theoretical analysis of the modal properties of stripe waveguides is more complex than for planar guides because of the extra dimension. A number of analytic techniques have been developed, but the solutions are cumbersome and restricted to simple cases[5]. More useful results have been obtained by numerical techniques such as the Beam Propagation Method (BPM) which can be applied to complex waveguide designs[9]. However, a simple method which gives some useful results and is reasonably accurate for characterising waveguides is the "effective index" method, described below[10].

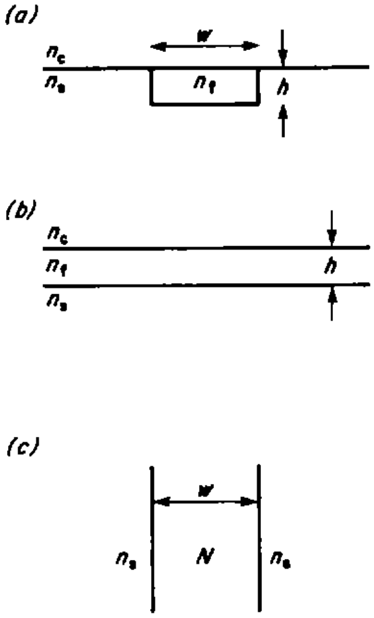

Fig. 6 — A schematic representation of the "effective index" method for analysing a stripe guide in terms of two orthogonal planar guides.

a) An embedded stripe guide
b) Step 1 : a planar guide, thickness h, index n_f
c) Step 2 : a planar guide, thickness W, index N

Consider the stripe waveguide shown in Fig. 6(a). The structure of the guide can be separated into two orthogonal planar guides (Figs. 6(b) and 6(c)). The planar guide in Fig. 6(b) is considered first and, an effective index calculated using the standard dispersion curves described in the previous Section. The value of the effective index is then inserted into the second planar guide structure (Fig. 6(c)), and the effective index and V value for the stripe guide is found using a second set of curves. The method can be applied to a variety of waveguide index profiles.

As in the case of planar guides, the number of modes can be controlled by varying the structure of the guide. For example, the film thickness, stripe width, and index difference can be tailored to give the desired result. Often it is required that the guide is single-mode to make a switch which, for example, relies on coupling between the fundamental modes of adjacent guides. As an example, a single-mode stripe waveguide formed by titanium indiffusion in lithium niobate (Section 3.2.1) has $n_s = 2.22$, $\Delta \simeq 0.01$, $h = 0.5-1.0$ μm, and $W = 5-8$ μm at a wavelength of 1.3 μm. It should be noted that as the wavelength is increased the guide dimensions are increased. Hence working at a longer wavelength eases the fabrication tolerances.

In more rigorous analyses of stripe guides, each mode has a different optical field distribution, and the dispersion curves are different for the TE and TM mode groups, as was the case for planar guides.

In addition to the scattering losses described for planar waveguides, stripe waveguides can lose optical power by radiation from bends[5]. The loss increases as the bend radius decreases. The loss can be minimised by increasing the refractive index difference, Δ. Bend loss is considered in more detail in Section 5 on switch arrays.

An additional point to note is that an optical fibre is functionally the same as the stripe waveguides discussed above, except that it has circular symmetry rather than rectangular. Consequently, the ideas of modes and V numbers also apply to fibres, apart from slight differences in definitions and dispersion curves. However, optical fibres are outside the scope of this Report and will not be discussed further.

3. Materials and fabrication techniques

Optical waveguides have been fabricated in a wide range of materials such as glasses, plastics, crystals and semiconductor materials[5]. The choice of material depends on the application. For instance, if the device is an active element such as a switch, the substrate will need to exhibit the electro-, acousto, magneto- or thermo-optic effects to allow an electrical signal to interact with the optical field. The first two effects are the most commonly used for high-speed, low-power active devices. Furthermore, if the device is to be single-mode, the index difference Δ should not be too large or else the dimensions of the device become too small to be fabricated easily (Equation 6). This Section describes the materials most commonly used.

Planar waveguides are the simplest to fabricate as the composition of the material has to be controlled in only one dimension. The fabrication of stripe waveguides is more complicated as the lateral dimension has to be controlled as well, this dimension being typically in the range 5–10 μm. A further complication is that integrated optical devices are typically 5–20 mm long, which means that the aspect ratio is greater than 1000. The specific techniques used to achieve such structures will be discussed in the following Sections.

3.1. Glass waveguides

Waveguides can easily be made in glass by immersion in ionic melts such as silver nitrate[11]. The silver ions exchange with the sodium ions in the glass to give a relatively large increase in index of $\Delta \simeq 0.1$. Consequently, it is a useful technique for fabricating multimode rather than single-mode guides.

As glass is an amorphous material it does not exhibit the electro- or acousto-optic effects. It is therefore mainly used for fabricating passive multi-mode devices such as power splitters or combiners[12]. However, the thermo-optic effect has been utilised for making slow (msec) switches[13].

3.2. Lithium niobate ($LiNbO_3$) waveguides

This crystal is the most commonly used substrate material for active integrated optical devices. It exhibits large electro- and acousto-optic effects which means that efficient switches and modulators have been made which require low voltages ($<5\,V$)[14]. There are two main fabrication techniques used with this material, namely titanium indiffusion and proton exchange.

3.2.1. Titanium indiffusion in lithium niobate

In this process, a layer of titanium, typically 30 nm thick, is evaporated on to the crystal substrate. The sample is then baked in an argon atmosphere at 1000°C for 5–10 hours which causes the titanium to diffuse into the crystal lattice, raising the refractive index[15]. The index profile is approximately Gaussian, with a peak increase in refractive index of $\Delta \simeq 0.01$. Stripe waveguides can be made by diffusing stripes of titanium which have been photolithographically defined (Appendix 1). As the index difference is low, it is reasonably easy to fabricate stripe widths of 3–8 μm for single-mode guides. Care has to be taken in the processing to avoid out-diffusion of lithium oxide which can give rise to an unwanted planar guide.

Waveguides fabricated by the titanium indiffusion technique guide both TE and TM polarisations, and can have propagation losses of less than 0.3 dB/cm[16]. Furthermore, by careful adjustment of the waveguide cross-section it has been demonstrated that coupling losses (fibre-waveguide-fibre) as low as 1 dB are possible[17].

A disadvantage of waveguides fabricated by this method is that they are prone to optical damage which distorts the refractive index difference of the guide for optical power levels above about 1 μW/μm^2 at a wavelength of 633 nm.[18]. However, at longer wavelengths the damage threshold is increased[19]. At 1.3 μm, the threshold is two to three orders of magnitude higher[16]. Further improvements can be achieved by using magnesium-doped lithium niobate[20], or annealing the waveguide[21].

The electrode structures required for active devices are fabricated on top of the waveguides by a further photolithographic process. Because the guides are narrow, and the aspect ratio is large (>1000), precision alignment devices are required.

3.2.2. Proton exchange in lithium niobate

In this process, the high index layer is formed by immersing a substrate in molten benzoic acid (T=250°C) for several hours[22]. The protons exchange with the lithium ions to give an index profile which is close to an ideal step function, with a peak index increase of $\Delta \simeq 0.13$. Annealing of the exchanged guides at elevated temperatures allows the index profile to be modified to a Gaussian form if desired[23]. It is possible to reduce the peak index change to $\Delta \simeq 0.01$ by buffering the acid melt using lithium benzoate[23]. The smaller index change means that single-mode stripe guides can be fabricated.

It has been found that aluminium can be used as a mask for defining stripe waveguide patterns. The mask can also be used as the electrode structure in active devices.

Guides fabricated by proton exchange do not suffer from optical damage. However, it has been found that applied static electric fields cause the index profile to drift with time, which limits the usefulness of this fabrication technique for making active devices which require static biassing[24]. Furthermore, the guides will only support one polarisation, as the process gives an increase in index along only one of the axes of the crystal. This restriction can limit the flexibility of device design.

It has been reported that a combination of these two processes gives guides which combine their best qualities[22]. The composite process (titanium indiffusion, proton-exchange or TIPE) produces guides which support both polarisations, and have a high optical damage threshold.

3.3. Semiconductor waveguides

There has been much interest recently in the use of these materials for integrated optics because of the potential for complete integration of sources, detectors, and switches/modulators on a common substrate. Consequently, the development of devices using these materials is rapidly catching up with lithium niobate technology. Nearly all of the types of active devices made in lithium niobate have also been made in semiconductor materials such as gallium arsenide (GaAs) and indium phosphide (InP). The performance of the semiconductor devices is similar to lithium niobate devices[25], although the two materials have different advantages and disadvantages. Some properties of the two materials are compared below.

(i) Lithium niobate has an electro-optic effect six times that of gallium arsenide. However, it is possible to offset most of the reduced efficiency of gallium arsenide by optimising the overlap of the electrical and optical fields by careful control of doping and composition.

(ii) Lithium niobate is an insulator, and therefore it is possible to apply fields in different directions on the same substrate. As gallium arsenide is a semiconductor this is more difficult.

(iii) Lithium niobate is very birefringent (i.e. it has different refractive indices for different polarisations in the crystal). Gallium arsenide has no bulk birefringence, but it can be introduced structurally if required.

(iv) The lowest loss reported in gallium arsenide is about three times that in lithium niobate, but it should decrease as processing techniques improve.

(v) There are no problems of optical damage or field-induced drift in gallium arsenide as there are with lithium niobate.

(vi) Lithium niobate devices are relatively easy to fabricate although the process is not well understood. Gallium arsenide devices are currently difficult to make and expensive, but they have the potential for good control, high yield, and flexibility in design.

The fabrication of semiconductor integrated optical devices uses standard photolithographic techniques to delineate the waveguide patterns (Appendix 1). The waveguide structure is commonly a ridge guide (Fig. 5(c)). More advanced structures use doping and compositional control to grow embedded guides (Fig. 5(b)).

4. Switches

There are many integrated optical switch designs based on a variety of materials and properties[5]. Switches have been designed for planar geometries, as well as single– and multimode stripe guides.

The most useful are those made from lithium niobate and semiconductor materials such as gallium arsenide. In general, switching is achieved by the interaction of the optical field with an electrical (or acoustic) field, generated by a suitable electrode structure on the surface.

The performance of optical switches can be characterised by a number of parameters, such as extinction ratio, insertion loss, drive voltages, bandwidth and polarisation sensitivity. One of the most important is the extinction ratio, to be defined in Section 4.1. If the extinction ratio is poor, the signal-to-noise ratio (SNR) of the wanted signal is degraded by cross-talk from the unwanted channels[26]. The problem becomes worse as more switches are combined in arrays. (However, reported values for the extinction ratio can be misleading as the ratio depends on the switching efficiency and straight-through transmission efficiency. Consequently, the extinction ratio is often different for each of the switch outputs).

The insertion loss is very important in an optical system, because there is generally a limited power margin[2]. Consequently, with high insertion loss, fewer switches can be used in a system. Because multimode stripe guides are shallow to allow a good overlap between the optical and electric fields, the insertion loss is high between circular cross-section multimode fibres and shallow, rectangular waveguides. In comparison, the refractive index profile of single-mode waveguides can be accurately matched to single-mode fibres, giving a low insertion loss. Accordingly, single-mode switch designs are the most important as it is possible to obtain low overall losses in optical fibre systems.

Ideally, switches should be polarisation-independent. However, if switches are dependent on polarisation, the optical fibre used in a system would have to be polarisation-maintaining, with the associated cost penalties, and increased complexity of installation. Alternatively, polarisation controllers could be used (Section 6.3).

The bandwidth is not generally critical, as most switching operations can be relatively slow i.e. tens of milliseconds. However, for some applications it might be desired to be able to switch in a television field-blanking period (i.e. about 1 msec).

The drive voltage requirement is reasonably important, with the main restriction being that the switching voltages should be within operational amplifier output levels to facilitate circuit design.

In summary, single-mode switches are the most important because of the need for low insertion loss. Two particular designs, the X-type and the directional coupler have been studied in some detail, and are the most promising. They are described in Sections 4.2 and 4.3 respectively.

Before describing the two designs, the definition of extinction ratio will be discussed.

4.1. Definition of extinction ratio

Consider the elementary two-way changeover switch shown in Fig. 7. It has two states, the bar and cross states (Fig. 7(a) and 7(b) respectively). In the bar state, most of the input light goes straight through (a fraction α_1). In the cross state, most of the light is switched into the other output (a fraction α_2). It is assumed that there is a propagation loss through the switch, such that a fraction γ of the input power is transmitted to the outputs. The extinction ratios for the two states are then defined as (see Appendix 2 for a detailed analysis):

$$R(\text{bar}) = (1 - \alpha_2)/\alpha_1 \qquad (10)$$

$$R(\text{cross}) = (1 - \alpha_1)/\alpha_2 \qquad (11)$$

It should be noted that if $\alpha_1 \simeq 1$, then R(bar) can be high i.e. poor extinction ratio, if the switch efficiency α_2 is low. For example, if α_1 = 99% and α_2 = 90%, then R(bar) and R(cross) are −10 dB and −19 dB respectively. It can therefore be misleading if only R(cross) is quoted for the performance of a switch.

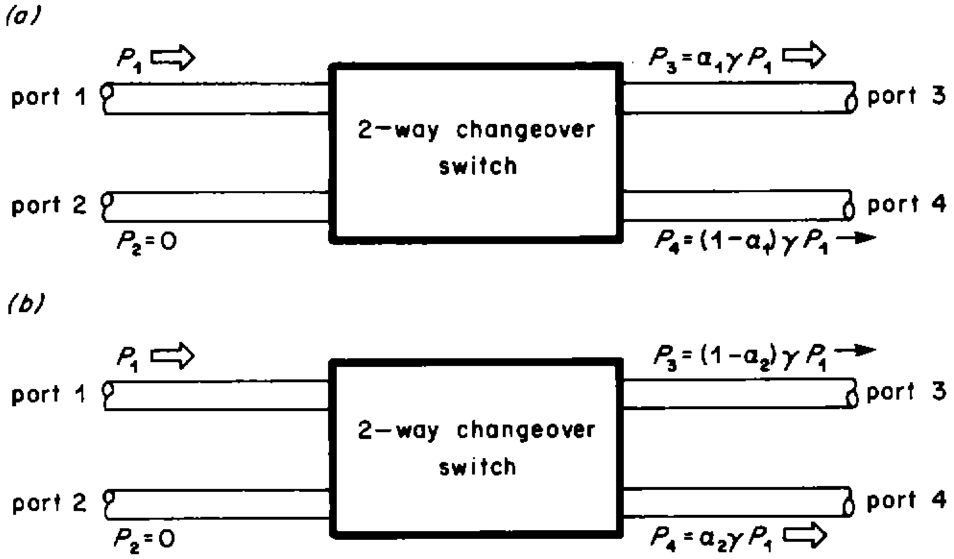

Fig. 7 – A basic 2-way changeover switch

a) The bar state
b) The cross-state

4.2. The X-type or cross-over switch

The simplest form of optical switch is the X switch shown in Fig. 8. It consists of two waveguides crossing at a small angle (1–2°). The two waveguides are fabricated in separate steps, so that the index difference in the intersection region is twice that of the guides. A pair of electrodes is aligned to bisect the angle, with the electrode separation, d, narrower than the guide width, W.

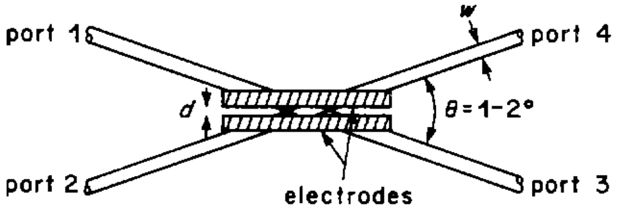

Fig. 8 – The X-type switch.

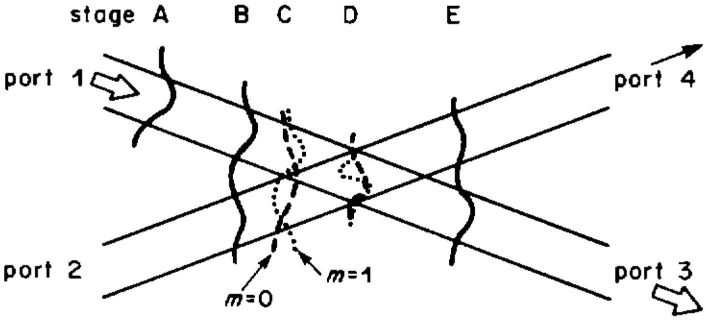

Fig. 9 – A schematic representation of the operation of an X-type switch.

Stage A :	Light is launched into the fundamental mode (m=0) of Port 1.
Stage B :	The light in Port 1 couples into the fundamental mode of Port 2.
Stage C :	The fundamental modes of Ports 1 and 2 convert to the symmetric, fundamental (m=0) mode and the asymmetric (m=1) mode of the intersection region.
Stage D :	The two modes propagate with different propagation constants.
Stage E :	The two modes convert to the fundamental modes of Ports 3 and 4, with the amplitudes depending on the relative phases.

The operation of the single-mode switch is shown schematically in Fig. 9 (the general principle also applies to multimode designs). Light launched into the fundamental mode of one of the input ports excites the symmetric (m=0) and antisymmetric (m=1) modes of the two coupled guides. The intersection region can support both of the modes because the V number is larger due to the increased index difference, (Equation 6). The difference in propagation constants β_s and β_a of the two modes leads to an oscillation of their relative phase along the propagation direction. At the end of the intersection region, the two modes convert to the fundamental (m=0) modes of the output guides. The amplitudes of the fundamental modes in the output guides depend on the relative phases of the modes in the intersection region. Consequently, the output amplitudes can be controlled by applying a voltage to the electrodes, which changes the refractive index in the intersection region via the electro-optic effect. The change in index alters the difference in propagation constants, and therefore changes the relative amplitudes at the outputs.

Extinction ratios of R(cross) = −23 dB and R(bar) = −10 dB have been reported for this type of switch[27]. The poor figure for R(bar) is due to the poor switching efficiency ($\alpha_2 \simeq 90\%$).

A major advantage of this type of switch is that it is compact, with the intersection region being about 200-500 μm long. Consequently, the electrode structure, and hence capacitance, is small, allowing high-speed operation. In addition, the small size means that a large number of devices can be included on a single substrate. If the extinction ratio can be improved, the X switch could be a useful design for large switch arrays.

In general the design is polarisation-sensitive as the operation of the switch depends on controlling the relative phase i.e. the difference in propagation constant of the lowest order modes. The propagation constants of these modes depend on the polarisation (Section 2.1), and the difference is not necessarily the same for the two polarisations.

The best reported characteristics of the X-type switch design are summarised in Table 1.

4.3. The directional coupler switch

A basic directional coupler is shown in Fig. 10, where two single-mode waveguides are in close proximity over a length D. If the separation, g, is small enough (typically 2-5 μm) such that the optical fields of the two guides overlap, light launched into one guide will begin to couple into the other guide. If the propagation constants β_1 and β_2 of the two guides are identical (i.e. $\Delta\beta = \beta_1 - \beta_2 = 0$), all the energy in one guide will be coupled into the other after a distance L (see curve (a) in Fig. 11). After a further distance L all the light will have coupled back again, unless the coupling is reduced, for instance, by increasing the separation of the guides.

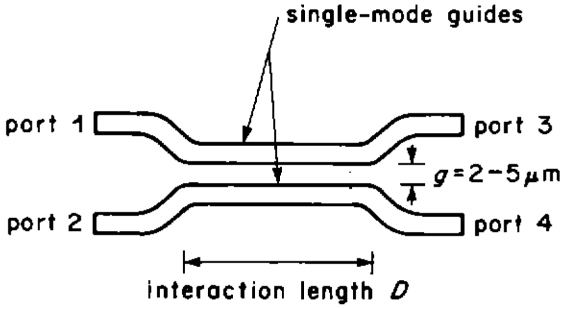

Fig. 10 – A directional coupler.

It is important to note that total transfer of energy between the guides depends critically

TABLE 1. Optical switches: the best reported performance figures

Parameter / Switch Design	Substrate material	R(cross) (dB)	R(bar) (dB)	Control voltage (V)	Bandwidth (GHz)	Insertion loss (dB)
X-type	Lithium niobate	−23 [27]	−10 [27]	12.5 [27]	6.0 (theoretical) [39]	not known
Stepped $\Delta\beta$ reversal directional coupler	Lithium niobate	−35 [29]	−35 [29]	4.5 [30]	6.0 (experimental) [31]	1.5 [36]
Stepped $\Delta\beta$ reversal directional coupler	Gallium arsenide	−16 [37]	−13 [37]	14 [37]	not known	not known

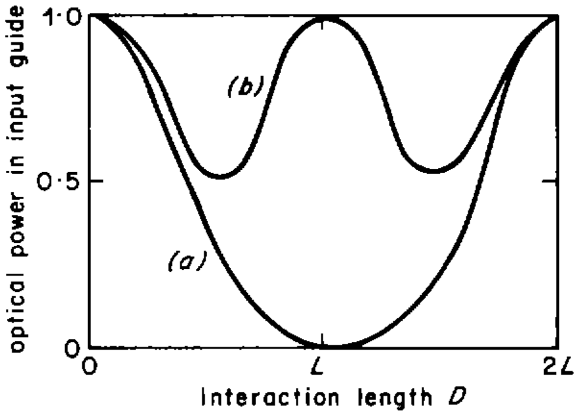

Fig. 11 – The optical power in one guide of a directional coupler as a function of the interaction length.

a) $\Delta\beta = 0$
b) $\Delta\beta \neq 0$

on the phase matching of the two guides i.e. $\beta_1 = \beta_2$. Since the relative propagation constants can be controlled through the electro-optic effect, it is possible to make a switch using a directional coupler by introducing a mis-match $\beta_1 \neq \beta_2$ between the two guides.

Such a switch is shown in Fig. 12 where a pair of electrodes have been fabricated above a directional coupler. The coupler is designed such that complete transfer (cross state) occurs for zero applied voltage. Application of a voltage to the electrodes causes a mis-match in the phase velocities, which prevents 100% transfer of energy. If the mis-match is adjusted to the appropriate value for the guide length, all the energy can be coupled back to the original guide (curve (b) of Fig. 11). This corresponds to the bar state. In theory, one could therefore make a perfect switch by this method.

Unfortunately, it is very difficult in practice to make a useful switch with this simple design. The problem lies with the conditions required for complete transfer of light from one guide to the other. Near 100% transfer (switching efficiency) can only be achieved if the interaction length D is exactly equal to the coupling length L. The latter cannot be controlled to any significant extent electro-optically, so electrical adjustment of the cross-state operating point is not possible. The coupling length depends primarily on the fabrication process. As the coupling length is exponentially dependent on the waveguide separation, the manufacturing tolerances required to make such a switch with acceptably low cross-talk is beyond current state of the art. Practical

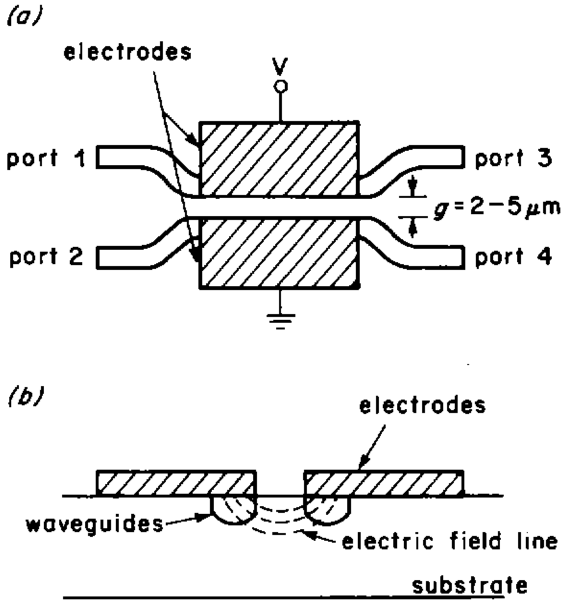

Fig. 12 – A schematic of a directional coupler switch showing the electrode structure.

a) Top view
b) Cross-section through the middle of the switch

extinction ratios usually quoted for this type of device are about in the range −10 to −15 dB.

Fortunately, however, it is possible to modify the directional coupler design such that the operating points can be adjusted electrically. Fig. 13 shows a "stepped $\Delta\beta$ reversal" coupler where the electrodes have been divided into two sections[28]. The cross-state is adjusted by the two

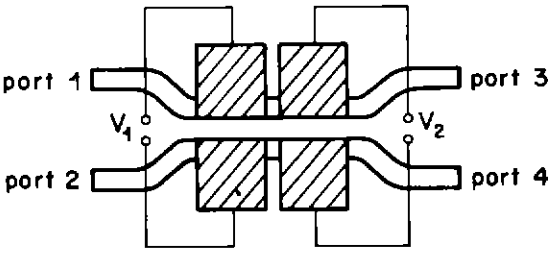

Fig. 13 – A stepped $\Delta\beta$-reversal directional coupler switch.

drive voltages of opposite polarity, and the bar-state is adjusted by the uniform bias applied to the whole switch. Extinction ratios of $R(\text{cross}) = R(\text{bar}) = -35$ dB have been reported for such devices made in lithium niobate[29], although at the cost of increased complexity.

The performance of this type of switch can be very good, with switching voltages as low as 4.5V[30], and operating speeds up to 6 GHz[31]. The best reported characteristics of directional coupler switches are also summarised in Table 1. It should be noted, however, that these characteristics cannot usually be achieved simultaneously in one device.

The major drawback with this type of device is that it tends to be long (typically 5-10 mm), which makes integration of many of these devices on to a single substrate difficult. Furthermore, the requirement for several independent voltages to be applied to each switch element to achieve optimum performance may be a problem in a large matrix.

In general, the directional coupler switch is polarisation sensitive, although it is possible to make polarisation-independent designs, at the cost of a further increase in complexity[32].

5. Switch arrays

Switch arrays can be divided into two separate types, blocking and non-blocking. In blocking arrays, the selection of one signal path can limit the other paths available. In non-blocking arrays, the signal paths are independent. The choice of array depends on the flexibility required.

Blocking arrays are useful where limited routing is required, for example in simple distribution systems or bypassing failed components. However, a studio centre routing system such as the one at the BBC Television Centre requires a non-blocking array for maximum flexibility. An additional requirement is that ideally each input can simultaneously feed all the outputs. At present, the switching array in the Central Apparatus Room can handle about 100 inputs and outputs. An integrated optical system would have to be able to switch at least as many channels, assuming that the configuration of studios and facilities were to remain unchanged in the transition to all-digital operation.

As in the case of isolated switches, there are a number of important characteristics of switch arrays which need to be considered. One of the most important is again the extinction ratio. As practical integrated optical switches have a finite extinction ratio, the signal-to-noise ratio (SNR) of the channel is degraded. If switches are combined in an array, the degradation is compounded at each device. The degraded SNR leads to a reduction in the overall performance of the system and, ultimately, can limit the maximum size of an array. It has been found that a SNR of 10 dB gives a reduction in the optical power margin of 1 dB[26].

Secondly, the fibre-substrate-fibre insertion loss needs to be low if a number of substrates are required to make up a large array. The latter is likely to be the case as most integrated optical devices are long (typically 3-10 mm), and the largest commercial substrates are only 75 mm long. Although insertion losses as low as 1 dB have been reported for single fibre connections[17], it is unlikely that such low losses would be achievable in large arrays where many fibres have to be connected in parallel. Furthermore, the low loss was achieved by optimising the waveguide cross-section. Such a cross-section is not necessarily the optimum for switching voltage, or extinction ratio, for example.

A further complication arises from the need to connect each switch element together to form an array. Bends in optical waveguides tend to radiate power (see Section 2.1), and therefore represent another source of loss. Furthermore, the radiated power can aggravate cross-talk problems in adjacent devices. The bend loss decreases as the bend radius increases, so is a trade-off between packing density and loss. For example, it has been calculated that for typical single-mode titanium-indiffused guides in lithium niobate, a bend radius of >30 mm is required to obtain a loss of less than 1 dB/cm[16]. It is possible to reduce bend loss by increasing the index difference, Δ in the bend region[16]. However, this makes fabrication more complicated as the thickness of titanium has to be varied across the substrate, and in any case the maximum index difference is limited for single-mode operation. Alternatively, it has been reported that smaller radii can be made with reduced loss, using a coherent-coupling effect[33], although this has not yet been demonstrated in a switch array.

In addition to the bend loss, there are other considerations such as electrical cross-talk between adjacent switches which also limits the packing density[16].

Although non-blocking arrays are the most relevant to a studio centre distribution system, blocking arrays will be discussed first as there have been some experimental studies of these.

5.1. Blocking arrays

A number of small integrated optical blocking arrays have been reported, based on directional coupler and X-type switch elements. The performance of these designs is described in the following sub-sections.

5.1.1. Blocking arrays using directional coupler elements

The main results of the performance of two 4 x 4 arrays of the design shown in Fig. 14 are summarised in Table 2[16,34]. Both designs were based on reversed $\Delta\beta$ directional couplers using titanium-indiffused waveguides on lithium niobate.

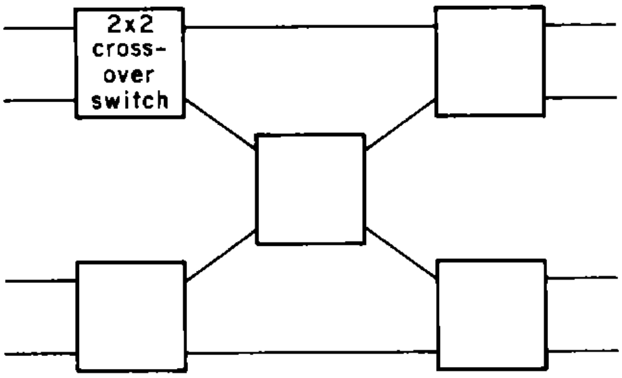

Fig. 14 – A 4x4 blocking switch array using reversed $\Delta\beta$ directional coupler switches.

TABLE 2. Summary of the performance of two 4 x 4 arrays

Parameter	Derived from Reference:	
	[34]	[16]
Minimum extinction ratio of the outputs of the array	−18 dB	−14 dB
Extinction ratio of the single elements	−26 dB	−18 dB
Switching voltages: cross	~25V	12V
bar	not known	25V
Insertion loss	not known	6.5 dB
Length of device	~30 mm	40 mm

There are several points to note from these results. Firstly, the extinction ratio for the whole array is reduced by 4-8 dB, with respect to single switch elements. This degradation is due to the compounding of the cross-talk from each switch, and the difficulty of optimally biassing each switch element. These problems would become worse as the array size increased.

Secondly, the devices were 30-40 mm long which demonstrates the low packing density due to the long switch elements, and the need for a minimum bend radius in the connecting guides.

Thirdly, the insertion losses were high because the input/output fibres were aligned simultaneously using a vee-groove technique. Even so, this technique is likely to be used for fabricating large arrays, as it is not practical to align each fibre individually.

5.1.2. Blocking arrays using X-type switch elements

A blocking array has been reported which used six X-type switch elements in a routing/monitoring circuit for data transmission (Fig. 15)[35]. The performance is summarised in Table 3.

TABLE 3. Performance of a blocking array using X-type switches

Extinction ratios for the elements in the array	−15 dB to −32 dB
Switching voltages : cross	−11V to −18V
bar	10V to 16V
Insertion losses	4.1 dB to 6.9 dB
Length of switch array	~25 mm

The main point to note is that although the X-type switch elements are much shorter than directional coupler switches, the array length is only slightly shorter. This is because the overall length is primarily determined by the bend losses of the connecting guides, and the need to separate the switch elements to avoid interactions.

However, by comparing Figs. 8 and 13, it is apparent that the electrical biassing of X-type switches is more straightforward than reversed $\Delta\beta$ switches. Accordingly, large X-type switch arrays will be simpler to implement in practice.

5.2. Non-blocking switch arrays

There have been no reported experimental results of non-blocking, integrated optical arrays. However, it is possible to calculate a maximum array size from published data.

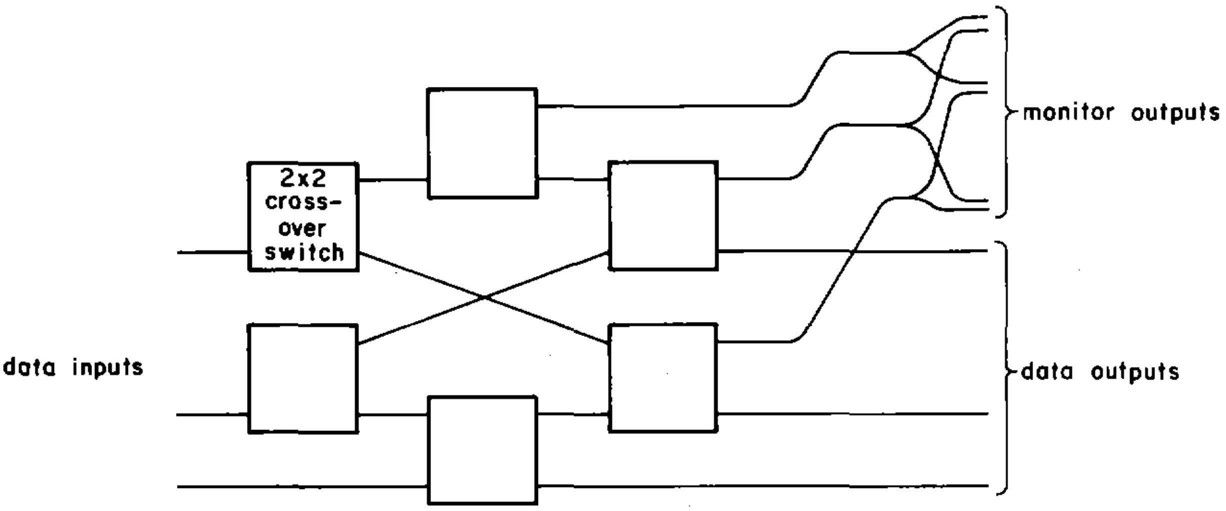

Fig. 15 – An optical data monitoring circuit using an array of six X-type switches.

A partial-tap, non-blocking switch array is shown schematically in Fig. 16. A conventional optical design for an element in such an array uses two mirrors, one partially-reflecting and the other totally-reflecting (Fig. 17). The partially-reflecting mirror is always in the input beam, with the tapped beam being directed to the output by raising the half-height, totally-reflecting mirror into position. The two-mirror design has the advantage of not affecting the input beam intensity during switching, and was used in the electro-mechanical switch array developed in the BBC Research Department[4].

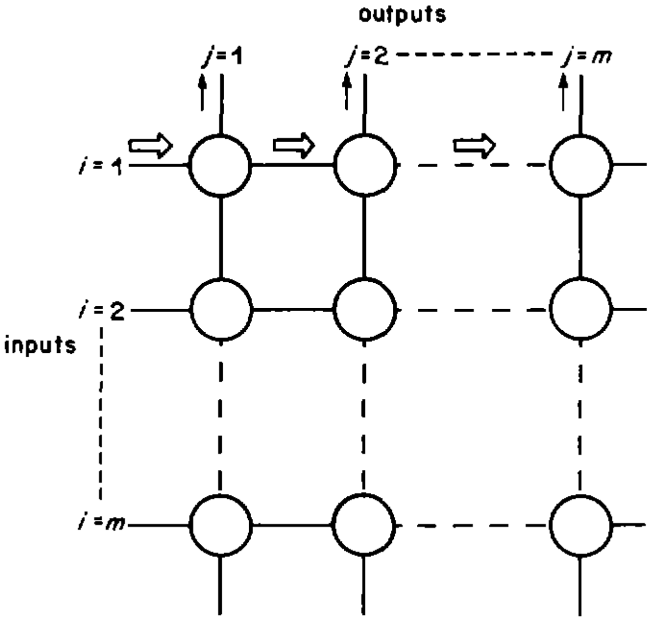

Fig. 16 – A schematic diagram of an M x M partial-tap, non-blocking switch array.

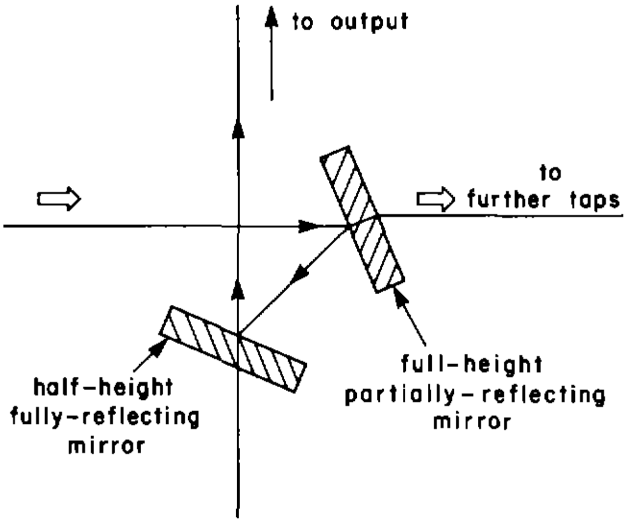

Fig. 17 – A two-mirror, partial-tap switch element.

The reflectivity of the partially-reflecting mirror needs to be different for each column of elements to keep the absolute power in each output equal. For an $M \times M$ array, the mirrors in column j should ideally have a reflectivity given by:

$$T_j = 1/(M + 1 - j) \tag{12}$$

where j is an integer of value $1 \leqslant j \leqslant M$

These same principles can be used to construct a non-blocking array using integrated optical switch elements. Furthermore, a partial-tap switch array of X-type switches can be designed which takes advantage of the extinction ratio R(cross), which is better than R(bar).

5.2.1. X-type switch elements in non-blocking, partial-tap arrays

Fig. 18 is an integrated optical equivalent of Fig. 17. (The angles in Fig. 18 have been exaggerated for clarity). The partially-reflecting mirror has been replaced by a coupler section C, which couples a fraction of the input light into the X-type switch S. The switch S can then be used to switch the selected signal into the output guide. The switch is characterised by a straight-through transmission efficiency α_1 and a switching efficiency α_2, as described in Section 4.1.

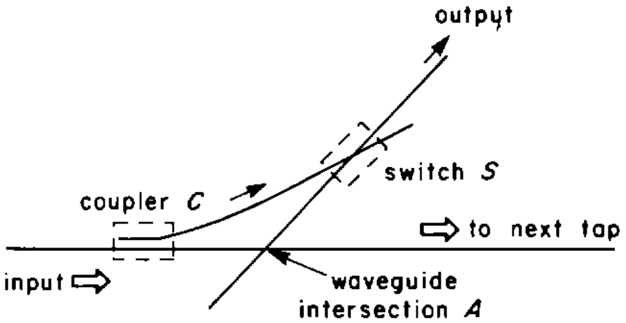

Fig. 18 – An integrated optical partial-tap switch element using a directional coupler and an X-type switch.

The input and output guides intersect at the point A. The intersection will have a finite cross-talk level from the input to the output, because of coupling between the guides in the intersection region[40], and scatter from defects[8]. It is assumed that the cross-talk into the output guide is a fraction $(1-\alpha_3)$ of the power in the input guide. In practice, the intersection angle would be chosen to minimise the cross-talk, bearing in mind that the cross-talk tends to decrease with increasing angle (with a superimposed periodic response[38]. However, a large angle would reduce the packing density, because the radius of curvature of the connecting guides needs to be a minimum value to keep bend losses low. Consequently, the design would have to be a compromise between cross-talk, bend loss and packing density.

As in the electro-mechanical design, the power level in the input guide of each element is constant irrespective of the state of preceding elements. It can be seen by comparing Fig. 18 with Fig. 7 that the switch S is used to take advantage of the extinction ratio R(cross), which is better than R(bar).

The signal-to-noise ratio (SNR) at the outputs of the M x M array can be determined by calculating the levels of the wanted and unwanted signals, assuming no propagation losses (Appendix 3). The SNR is given by:

$$\mathrm{SNR} = \frac{\{\alpha_2 + (1-\alpha_2)(1-\alpha_3)(M-1)\}\{1-\alpha_1\,\alpha_3\}}{\{1-\alpha_1+\alpha_1(1-\alpha_3)(M-1)\}\{(\alpha_1\alpha_3)^{(1-M)}-1\}} \quad (13)$$

Equation 13 is plotted as curve (a) in Fig. 19, showing SNR as a function of M, assuming the data for the X-type switches in Table 1. A cross-talk level of $(1-\alpha_3) = -30$ dB was assumed for the intersection A, which was optimistic[38]. The maximum size of array is limited by the acceptable SNR, which is assumed to be 10 dB[26]. It can be seen that the maximum size of the array is $M \simeq 8$.

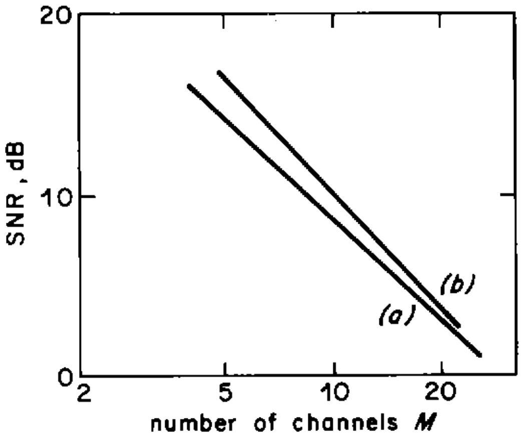

Fig. 19 – A graph of the signal-to-noise ratio of an integrated optical partial-tap, non-blocking switch array as a function of the number of channels, M.

a) The coupler/switch partial-tap element :

R(cross) = −23 dB
R(bar) = −10 dB
$(1-\alpha_3)$ = −30 dB

b) The double-switch partial-tap element :

R(cross) = −30 dB
R(bar) = −10 dB
$(1-\alpha_3)$ = −30 dB

It is possible to reduce the cross-talk level by modifying the switch element (Fig. 20). The coupler has been replaced by a second X-type switch S_2, which has the same characteristics as switch S. It is assumed that S_2 is in the off or bar state when the input is not selected. In this case the SNR is given by:

$$\mathrm{SNR} \doteq \frac{1}{M} \frac{\left\{\alpha_2 + (1-\alpha_2)(1-\alpha_3)(M-1)\right\}\left\{1-\alpha_1\alpha_3\right\}}{\left\{(1-\alpha_1)^2 + \alpha_1{}^2(1-\alpha_3)\right\}\left\{(\alpha_1\alpha_3)^{(1-M)}-1\right\}} \tag{14}$$

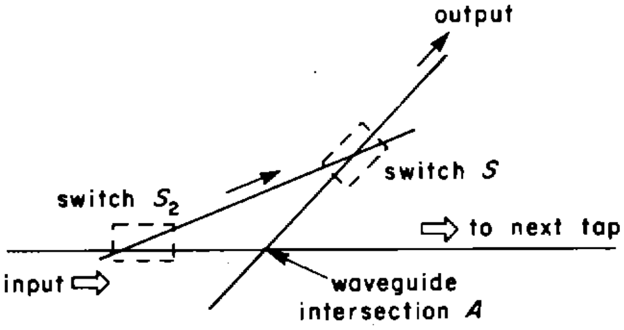

Fig. 20 – An integrated optical partial-tap switch element using two X-type switches.

Equation 14 is plotted as curve (b) in Fig. 19, which shows that the array size has been increased to $M \simeq 10$ for an SNR of 10 dB.

Improving the switch extinction ratio to −30 dB (which should be possible[27]) does not increase the array size. In fact, the array size is primarily limited by the intersection cross-talk. To increase the array to $M=100$, the intersection cross-talk would have to be improved to −50 dB.

It is unlikely that such an improvement will be achieved simply by developing current fabrication techniques. What is more likely to give the necessary improvement is the development of three-dimensional integrated optical devices, where the waveguides are buried in the substrate, rather than being on the surface. This would allow waveguides to cross-over without interacting, hence minimising cross-talk. However, such techniques are still in their infancy[40].

Alternatively, regenerators could be used between small sub-arrays to restore the data. Such a technique might be particularly applicable to semiconductor integrated optics, where the necessary opto-electronic components could be included on the same substrate. However, the technology is still being developed, and the eventual likely cost is uncertain.

6. Modulators and other devices

This Section describes a number of integrated optical devices (other than switches), which are of interest in optical communications systems. The devices described are phase and frequency modulators, a polarisation controller and tunable optical filters. It should be noted that although the main application for switches is for signal routing, switches can also be used for amplitude modulation.

6.1. The phase modulator

The simplest modulator is the phase modulator shown in Fig. 21. It consists of a single-mode waveguide with a pair of electrodes on the surface of the substrate. An applied voltage changes the refractive index difference of the guide via the electro-optic effect. The change in index alters the propagation constant β, which induces a phase shift in the transmitted light. The voltage required to induce a given phase shift depends on a number of parameters, such as device length, electro-optic coefficient of the substrate, and degree of overlap between the optical and electrical fields. Typically, a voltage-length product of 5-10 V.mm for a π phase shift has been reported for this type of device[41].

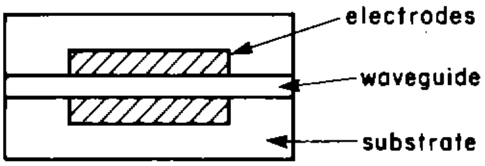

Fig. 21 – A phase modulator.

A phase modulator has obvious applications in PSK coherent transmission systems[42]. It is also possible to use a phase modulator as a frequency modulator by applying a linearly-increasing phase shift to the transmitted light. However, as it is not possible to increase the applied voltage indefinitely, an alternative is to use a sawtooth voltage waveform with a very short fall-time. This technique has been used to frequency shift optical signals by 25 MHz with spurious sidebands of <−16 dB[43].

6.2. The Mach-Zehnder interferometer (intensity and frequency modulator)

The Mach-Zehnder interferometer is shown in Fig. 22. Light launched into the input single-mode waveguide is split by the first Y junction. The light then travels along the two arms to the second Y junction where it is recombined. If the signals are equal and in phase, all the light is transmitted to the output guide. If the signals are in anti-phase the light is radiated into the substrate and no light is transmitted. The relative phase difference can be controlled by applying a voltage to electrodes positioned over the

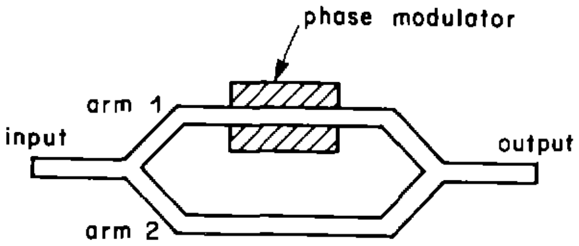

Fig. 22 – A Mach-Zehnder interferometer.

two arms of the interferometer. (This is simply the phase modulator described in the previous Section). Consequently, the transmitted intensity can be modulated by the applied voltage. Extinction ratios as good as −36 dB have been obtained[44].

The transmitted intensity varies sinusoidally with applied voltage, so a refinement to the design is to add a fixed $\pi/2$ phase offset to one arm by increasing its length[44]. The phase offset biases the output of the interferometer to its point of maximum linearity. A further refinement is to design the electrodes to allow travelling-wave operation i.e. to match the velocity of the optical signal to that of the microwave modulating signal. The best performance achieved so far is a bandwidth of 17 GHz[45].

The major use for Mach-Zehnder interferometers is likely to be in high bit rate (>1 Gbit/s) transmission systems. At these bit rates, the direct modulation of semiconductor diode lasers causes a time-dependent wavelength variation or "chirp"[46]. The dispersion of optical fibres causes the chirp to manifest itself as a reduction in the system bandwidth, particularly in advanced optical systems operating at 1.55μm where the fibre dispersion is not at a minimum. In general, the use of a constant output power laser source with a separate modulator is more promising for high bit rate systems.

Another use of the Mach-Zehnder interferometer is as a double sideband, AM, suppressed-carrier modulator. In this mode of operation the modulator generates two sidebands offset from the optical carrier by the modulation frequency. Two of these modulators can be used to generate a SSB signal which would be suitable for coherent optical transmission[47].

6.3. Polarisation controllers

In optical fibre communications, the term single-mode is often used incorrectly. In fact, a conventional single-mode fibre supports two orthogonally-polarised modes. The power in the two modes varies along the length of the fibre as stress-induced birefringence causes coupling between the two modes. This time/position-dependent power level can cause problems if there are polarisation-sensitive components in the system, and in extreme cases, the signal can fade completely. Examples of such components are some switches, modulators, and connectors/splices.

It is possible to control the polarisation of optical signals by electro-optically coupling the TE and TM modes of stripe waveguides. Because the two polarisation modes have different propagation constants (Section 2.1), a periodic electrode structure has to be used for phase matching (Fig. 23). Such a device is called a TE-TM mode converter. A conversion efficiency of >99% has been reported, with a drive voltage of ~2.5V for a 6mm long lithium niobate device[48]. Similarly, a gallium aluminium arsenide semiconductor device has been reported to give complete conversion, for a drive voltage of ~10V for a 1mm long electrode[49].

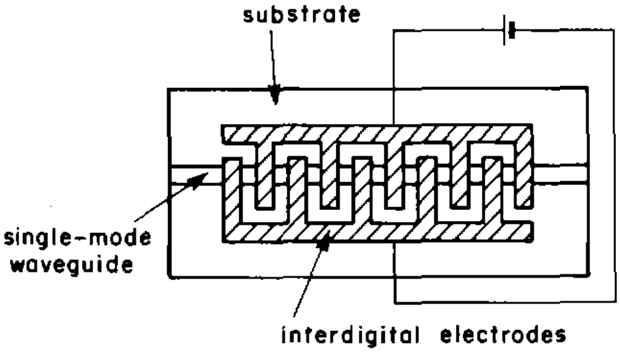

Fig. 23 – A polarisation-controller or TE-TM mode-converter.

6.4. Waveguide optical bandpass filters

Wavelength-division multiplexing (WDM) has the potential to increase the number of channels which can be carried on a single fibre[2]. Furthermore, it can perhaps be used as the basis for a large routing and distribution system, such as is envisaged for a future all-digital BBC Television Studio Centre, by obviating the need for switching[2]. Consequently, there is much interest in optical bandpass filters.

Integrated optical filters for use in a large (100 x 100) routing and distribution system would need to satisfy a number of requirements. These include low insertion loss, tunability of the filter pass-band, polarisation-insensitivity, high out-of-band rejection and an optical bandwidth of $\sim 1\,\text{nm}^2$. In fact, there have been no integrated optical filters reported so far which satisfy all of these requirements. However, three filter designs are described below to illustrate some of the possible techniques.

The three designs are the corrugated waveguide or grating filter, the wavelength-selective TE-TM mode converter and the directional coupler filter. The characteristic filter spectral bandwidths are shown in Fig. 24[50].

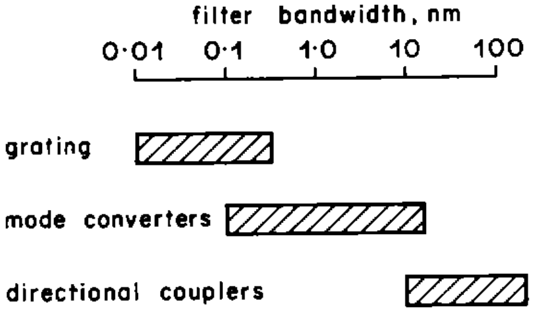

Fig. 24 — Characteristic filter spectral bandwidths of grating, mode-conversion and directional coupler filters.

Grating filters make use of the wavelength dependence of the Bragg effect. The grating or corrugation on the surface of the substrate scatters some of the power from the guided mode. For a corrugation of period ω, the guided mode is strongly reflected for a wavelength λ which satisfies the phase matching condition:

$$\lambda_o = 2N\omega \qquad (15)$$

where N is the effective index (Section 2.1). A filter bandwidth as low as 0.01 nm has been demonstrated for a 10 mm long glass waveguide[51]. However, the device is limited in usefulness because it is not easily tunable.

A TE-TM mode converter fabricated in a birefringent material such as lithium niobate is naturally wavelength-selective because of the requirement for phase matching to give high conversion efficiency. Using electrode lengths from 0.5 to 6 mm, filter bandwidths of 5 to 0.5 nm have been demonstrated[48]. In the same study, a three-channel device was fabricated, with a channel spacing and bandwidth of 8 nm and 1.5 nm respectively. The measured crosstalk was ~20 dB. In another study, the filter response was tuned by varying the substrate temperature, with a coefficient of ~1 nm/°C[52]. However, the major disadvantage of the mode-converter is that the filter response is a (sinx/x) function of wavelength, which gives insufficient out-of-band rejection for a multichannel WDM system.

Broad-band filtering can be achieved using a specially designed directional coupler (Section 4.3). If the two waveguides in the coupling region are of different widths and thickness, the dispersion curves are not the same (Fig. 25(a)). Consequently, appreciable coupling only occurs at the phase-matched wavelength λ_{pm} (Fig. 25(b)). By applying a voltage to the electrodes, the reponse can be tuned to a different wavelength λ_{tpm}. For example, a filter has been demonstrated with a 3 dB bandwidth of 20 nm at $\lambda = 600$ nm[53]. The filter could be tuned over 60 nm. However, the bandwidth of directional coupler filters in general is too large (>10 nm), and the filter is polarisation-sensitive.

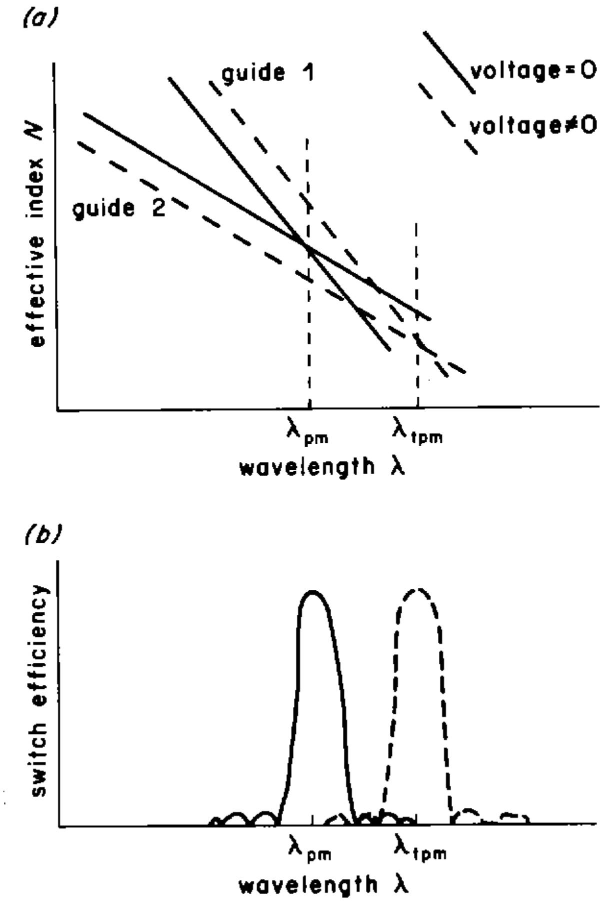

Fig. 25 — a) the dispersion curves of the two guides of the directional coupler filter (with and without an applied tuning voltage). b) The switch efficiency of the directional coupler filter as a function of wavelength.

7. Conclusions

The basic principles of integrated optical waveguides have been discussed. Particular emphasis is placed on the idea of possible modes of propagation, and how the characteristics of different waveguides can be related by a set of normalised equations. The most common materials and fabrication techniques are described, and their advantages and disadvantages discussed.

The most important potential application of integrated optics in the context of broadcast engineering is for routing digital optical signals distributed by optical fibres. Therefore, the operation and performance of the two most promising switch designs are described and compared in some detail. The main conclusion is that the X-type switch is likely to be the best choice for use in a switch array.

The main requirement envisaged for the all-digital routing and distribution system in the BBC Television Centre is likely to be for a large (100 x 100) partial tap, non-blocking switch array. The design of such an integrated optical non-blocking array using X-type switches is discussed.

The main conclusion is that the main limitation on the maximum array size is the cross-talk at the intersections of the interconnecting waveguides. With the present technology, cross-talk limits the maximum array size to ~10 x 10. Improvements of up to 20 dB will be required to make 100 x 100 integrated optical non-blocking arrays. Such improvements are only likely to be achieved by the development of fabrication techniques to allow waveguides to be buried below the substrate surface. Alternatively, regenerators could be used between small sub-arrays to restore the data signal-to-noise ratio.

8. References

1. CCIR Recommendation 601. 1983. Encoding parameters of digital television for studios.
2. MARSDEN R.P., WILLSON J.P., *and* ZUBRZYCKI J.T. 1985. Digital television routing systems: a survey of optical and electrical techniques. BBC Research Department Report in course of preparation.
3. MARSDEN R.P. 1983. Optical fibre links for digital YUV signals. BBC Research Department Report No. 1983/14.
4. ZUBRZYCKI J.T. *and* MARSDEN R.P. 1985. Digital television routing systems: an experimental optical switching matrix. BBC Research Department Report in course of preparation.
5. HUNSPERGER R.G. 1984. Integrated optics: Theory and Technology. Springer Series in Optical Sciences Vol. 33. Springer-Verlag. Berlin.
6. TAMIR T. (ed.) 1979. Integrated optics. Springer Topics in Applied Physics Vol. 7. Springer-Verlag. Berlin.
7. HOCKER G.B. *and* BURNS W.K. 1975. Modes in diffused optical waveguides of arbitrary profile. *IEEE J. Qu. El.* **QE-11**, pp 270-276.
8. ARMENISE M.N., DE SARIO M., CANALI C., FRANZOSI P., SINGH J., HUTCHINS R.H., *and* DE LA RUE R.M. 1984. In-plane scattering in titanium-indiffused Ti:LiNbO$_3$ optical waveguides. *Appl. Phys. Lett.* **45**, pp 326-328.
9. FEIT M.D. *and* FLECK J.A. 1980. Computation of mode properties in optical fibre waveguides by a propagating beam method. *Appl. Opt.* **19**, pp 1154-1164.
10. HOCKER G.B. *and* BURNS W.K. 1977. Mode dispersion in diffused channel waveguides by the effective index method. *Appl. Opt.* **16**, pp 113-118.
11. WALKER R.G., WILKINSON C.D.W., *and* WILKINSON J.A.H. 1983. Integrated optical waveguiding structures made by silver ion-exchange in glass. *Appl. Opt.* **22**, pp 1923-8.
12. OKUDA E., ICHIRO T., *and* YAMASAKI T. 1984. Planar gradient index glass waveguide and its application to a 4-port branched circuit and star coupler. *Appl. Opt.* **23**, pp 1745-8.
13. HARUNA M., *and* KOYAMA J. 1982. Thermo-optic deflection and switching in glass. *Appl. Opt.* **19**, pp 3461-3465.
14. ALFERNESS R.C., KOROTKY S.K., BUHL L.L., *and* DIVINO M.D. 1984. High-speed, low-loss, low-drive power travelling wave optical modulator for 1.3 μm. *Elec. Lett.* **20**, pp 354-5.
15. SCHMIDT R.V., *and* KAMINOW I.P. 1974. Metal-diffused optical waveguides in lithium

niobate. *Appl. Phys. Lett.* **25**, pp 458-60.

16. KONDO M., OHITA Y., FUJURAWA M. *and* SAKAGUCHI M. 1982. Integrated optical switch matrix for single mode fibre networks. *IEEE J. Qu. El.* **QE-18**, pp 1759-65.

17. RAMASWAMY V., ALFERNESS R.C., *and* DIVINO M.M. 1982. High efficiency single mode fibre to lithium niobate waveguide coupling. *Elect. Lett.* **18**, pp 30-31.

18. JACKEL J.L., OLSON M. *and* GLASS M. 1981. Optical damage resistance of monovalent ion-diffused LiNbO$_3$ and LiTaO$_3$ waveguides. *J.Appl. Phys.* **52**, pp 4855-4856.

19. HAMMER *and* NEIL. 1982. Observations and theory of high-power butt-coupling to LiNbO$_3$ – type waveguides. *IEEE Trans. Micro. Theo. and Tech.* **MTT-30**, pp 1739-1746.

20. BRYAN D.A., GERSON R., *and* TOMASKI A.E. 1984. Increased optical damage resistance in lithium niobate. *Appl. Phys. Lett.* **44**, pp847-8.

21. BECKER R.A. 1984. Thermal fixing of Ti-indiffused lithium niobate channel waveguides for reduced optical damage. *Appl. Phys. Lett.* **45**, 121-3.

22. JACKEL J.L. *and* HOLMES R.J. 1983. Recent advances in lithium niobate processing. Proc. 2nd Eur. Conf. on Integ. Opt. IEE Publ. No. 277.

23. DE MICHELI M., BOTINEAU J., NEVEU S., SIBILOT P., *and* OSTROWSKY D.B. 1983. Independent control of index and profiles in proton exchanged lithium niobate guides. *Opt. Lett.* **8**, pp 114-5.

24. WONG K.K. 1984. Integrated optical devices fabricated by proton exchange in lithium niobate. Proc. IERE Colloquium on Integrated Optics. June 1984. London.

25. RITCHIE S., HOUGHTON A.J.N., *and* RODGERS P.M. 1984. Waveguide devices in semiconductors. Proc. IERE Colloquium on Integrated Optics. June 1984. London.

26. ZUBRZYCKI J.T. 1985. Digital television routing systems: crosstalk and signal-to-noise ratio in optical fibre networks. BBC Research Department Report in course of preparation.

27. MEYER A. 1983. Electro-optic X switch using single mode titanium lithium niobate channel waveguides. *Elec. Lett.* **19**, pp 553-4.

28. KOGELNIK H., *and* SCHMIDT R.V. 1976. Switched directional couplers with alternating delta beta. *IEEE J.Qu.El.* **QE-12**, pp 396-401.

29. WILKINSON J.S. *and* WILSON M. 1983. Theoretical and experimental investigation of a stepped delta beta directional coupler having a high extinction ratio. Proc. 2nd European Conference on Integrated Optics. October 1983. Florence. IEE Pub. No. 227.

30. ALFERNESS R.C., KOROTKY S.K., BUHL L.L., *and* DIVINO M.M. 1984. High-speed, low-loss, low-drive-power travelling wave optical modulator for 1.32 μm. *Elec. Lett.* **20**, pp 354-5.

31. AURACHER F., SCHICKENTANZ D., *and* ZEIDLER K.H. 1984. High speed delta-beta reversal directional coupler modulator with low insertion loss for 1.3 μm. *J. Opt. Comm.* **5**, pp 7-9.

32. ALFERNESS R.C. 1979. Polarisation-independent optical directional coupler switch using weighted coupling. *Appl. Phys. Lett.* **35**, pp 748-750.

33. BECKER R.A. *and* JOHNSON L.M. 1984. Low-loss multiple branching circuit in Ti-diffused LiNbO$_3$ channel waveguides. *Opt.* Lett. **9**, pp 246-248.

34. SCHMIDT R.V. *and* BUHL L.L. 1976. Experimental 4 x 4 optical switching network. *Elec. Lett.* **12**, pp 575-577.

35. NAKAJIMA H., SAWAKI I., SEINO M., ASAMA K., HORIMATSUT., *and* MURAKAMI K. 1984. Integrated optical switching circuit using Ti: LiNbO$_3$ waveguide network. Proc. 7th Topical Meeting on Integrated Optics and Guided Wave Optics, pp TuA4-1 to TuA4-4.

36. ALFERNESS R.C., BUHL L.L. *and* DIVINO M.M. 1982. Low-loss fibre-coupled directional coupler modulator. *Elec. Lett.* **18**, pp 490-1.

37. BRANDON J., CARENCO A., MENIGAUX L., *and* RONDOT M. 1983. Double hetero-structure GaAs–GaAl$_x$Ga$_{(1-x)}$As rib waveguide directional coupler switch. Proc. 2nd European Conference on Integrated Optics. October 1983. Florence. IEE Pub. No. 227.

38. BERGMANN E.E., McCAUGHAN 1. *and* WATSON J.E. 1984. Coupling of intersecting Ti:LiNbO$_3$ diffused waveguides. *Appl. Opt.* **23**, pp 3000-3003.

39. TSAI C.S., KIM B., *and* EL-AKIRI F.R. 1978. Optical channel waveguide switch and coupler using total internal reflection. *IEEE J. Qu. El.* **QE-14**, pp 513-7.

40. KING G.D.H., BONE M.C., WEISS B.L. *and* WEEKS D.W. 1981. Ion-implanted optical waveguides in LiNbO$_3$. *Elect. Lett.* **17**, pp 897-899.

41. CROSS P.S., BAUMGARTNER R.A., *and* KOHER B.H. 1984. Microwave integrated optical modulator. *Appl. Phys. Lett.* **44**, pp 486-8.

42. HOUGHTON A.J.N., RODGERS P.M. *and* ANDREWS D.A. 1984. High performance GaAs–GaAlAs phase modulators for PSK optical fibre systems. *Elec. Lett.* **20**, pp 479-81.

43. WONG K.K. *and* WRIGHT S. 1981. An optical serrodyne frequency translator. Proc. 1st European Conference on Integrated Optics. September 1982. London. IEE Pub. No. 201.

44. BULMER C.H. *and* BURNS H.K. 1984. Linear interferometric modulators on lithium niobate. *J. Light. Tech.* **LT-2**, pp 512-22.

45. GEE C.M., THURMOUD G.D. *and* YEN H.W. 1983. 17 GHz bandwidth electro-optic modulator. *Appl. Phys. Lett.* **43**, pp 998-1000.

46. LINKE R.A. 1984. Transient chirping in single-frequency lasers: lightwave systems consequences. *Elec. Lett.* **20**, pp 472-474.

47. IZUTSU M., SHIKAMA S. *and* SVETA T. 1981. Integrated optical SSB modulator/frequency shifter. *IEEE J. Qu. El.* **QE-17**, pp 2225-7.

48. ALFERNESS R.C. *and* BUHL L.L. 1980. Electro-optic waveguide TE-TM converter with low drive voltage. *Opt. Lett.* **5**, pp 473-475.

49. McKENNA J. *and* REINHART F.K. 1976. Double heterostructure GaAlAs pn-junction-diode-modulator. *J. Appl. Phys.* **47**, p 2096.

50. ALFERNESS R.C. 1981. Guided wave devices for optical communication. *IEE J. Qu. El.* **QE-17**, pp 946-959.

51. SCHMIDT R.V., FLANDERS D.C., SHANK C.V. *and* STANDLEY R.D. 1974. Narrow-band grating filters for thin-film optical waveguides. *Appl. Phys. Lett.* **31**, pp 651-652.

52. BOOTH R.C., DAYMOND-JOHN B.E., STURGES P.E., *and* WILSON M.G.F. 1984. Temperature tuning of LiNbO$_3$ electro-optic waveguide TE-TM convertors. *Elec. Lett.* **20**, pp 1045-1047.

53. ALFERNESS R.C. *and* SCHMIDT R.V. 1978. Tunable optical waveguide directional coupler filter. *Appl. Phys. Lett.* **33**, pp 161-163.

54. HATZAKIS M., CANAVELLO B.J. *and* SHAW J.M. 1980. Single-step lift-off process. *IBM J. Res. Dev.* **24**, pp 452-460.

9. Appendices

9.1. Appendix 1 : Photolithographic techniques

Photolithography is essentially the transfer of a pattern from a mask on to a coated substrate. The substrate is then processed to produce the desired device.

The starting point is the mask. This is usually a glass substrate which has been coated with a metal film such as aluminium or chromium, and a layer of photosensitive material (photoresist). The desired pattern is transferred to the photoresist by photographic reduction techniques. Alternatively, the pattern can be directly drawn with an electron beam system. The unwanted metal film is then removed by etching. The completed mask can then be used to replicate the pattern on a number of substrates. The commonest replication technique is the "lift-off" process.

The lift-off process for the fabrication of titanium-indiffused waveguides is shown schematically in Fig. 26. The substrate is coated with a layer of photoresist approximately 0.5 μm thick. The mask is then brought into intimate contact, and the photoresist exposed through the mask (Fig.26(a)). The mask is then removed, and the exposed photoresist is dissolved by development.

A film of titanium is then evaporated over the whole substrate (Fig. 26(b)). The unwanted titanium is then removed by lifting it off using a suitable solvent to dissolve the unexposed photoresist (Fig. 26(c)). This leaves the desired pattern of titanium, which can then be diffused into the substrate to form the waveguide (Fig. 26(d)).

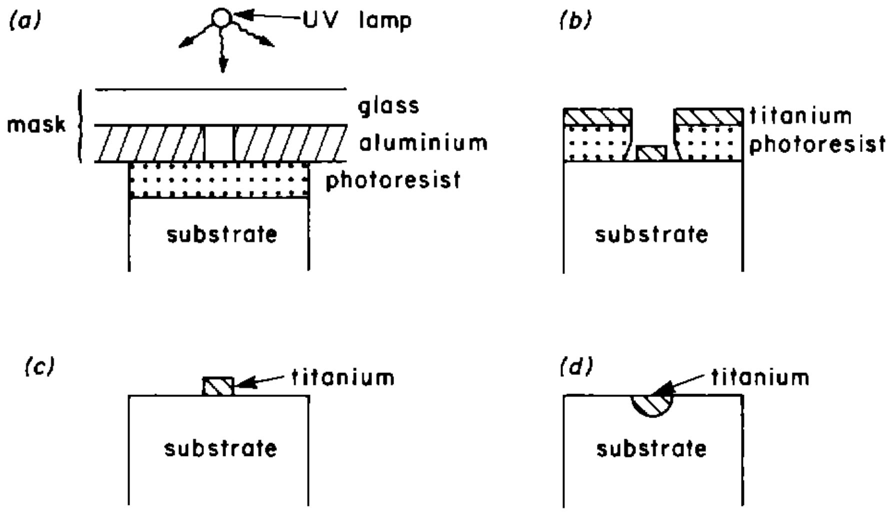

Fig. 26 — A schematic representation of the "lift-off" process for fabricating titanium-indiffused waveguides in lithium niobate.

a) Exposure of the photoresist
b) Development of the photoresist, and evaporation of the titanium film
c) Removal of the unwanted titanium film
d) Diffusion of the titanium into the substrate to form a waveguide.

The lift-off technique can be used to give linewidths of ~1 μm. However, it is important that there is an overhang at the edge of the photoresist after development, so that the evaporated titanium film does not form a contiguous layer (Fig. 27). This can be ensured by treating the surface of the photoresist prior to development with a solvent such as toluene[54] .

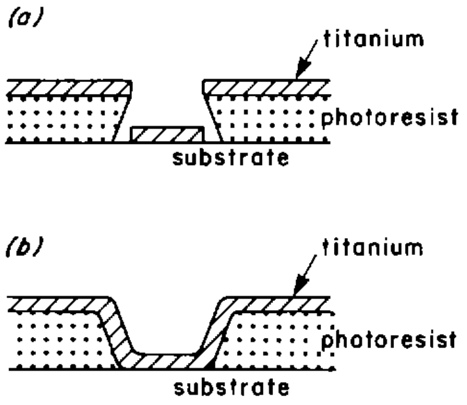

Fig. 27 — The "lift-off" process.

a) The formation of an overhang at the edge of the photoresist pattern gives a well-defined stripe of titanium.

b) With no overhang, the titanium film is contiguous, giving poor results when attempting to remove the unwanted titanium.

An alternative method is to coat the substrate with titanium, followed by a layer of photoresist (Fig. 28(a)). The photoresist is then exposed and developed to leave a ridge of photoresist over the titanium (Fig. 28(b)). Note that the mask is now the inverse of the mask used for the lift-off method. The unwanted titanium is then removed by etching (Fig. 28(c)). This method has the advantage that it is not critically dependent on forming an overhang in the photoresist. However, titanium is difficult to remove by chemical etching, and so expensive techniques such as reactive ion etching have to be used[25] .

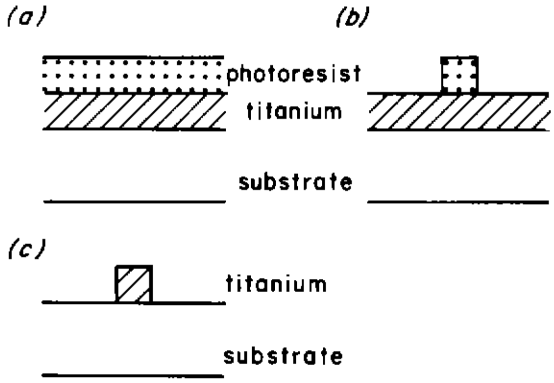

Fig. 28 — An alternative photolithographic process.

a) The substrate is coated with titanium and photoresist.
b) The resist is exposed and developed.
c) The unwanted titanium is removed by etching.

The alternative method is commonly used for fabricating semiconductor waveguides.

9.2. Appendix 2: Definition of extinction ratio

An ideal two-way change-over switch is shown in Fig. 7. It is assumed that an optical signal P_1 is launched into input 1, with no signal in input 2. We can define two states, the through or "bar" state, and the "cross" state. In the bar state, most of the input light (a fraction α_1) will exist from output 3. The optical powers from outputs 3 and 4 are then given by:

$$P_3 \text{ (bar)} = \alpha_1 . P_1 \tag{16}$$

$$P_4 \text{ (bar)} = (1 - \alpha_1). P_1 \tag{17}$$

assuming no loss in the switch. However, in a practical switch there will be some propagation losses due to scattering and radiation from bends (Section 2.2). Equations (16) and (17) therefore have to be modified to allow for a fraction $(1-\gamma)$ of the input light which is lost from the guides. Equations (16) and (17) then become:

$$P_3 \text{ (bar)} = \alpha_1 . \gamma . P_1 \tag{18}$$

$$P_4 \text{ (bar)} = (1-\alpha_1). \gamma . P_1 \tag{19}$$

As the bar state corresponds to the light travelling straight through the switch, α_1 will generally be close to unity. It will be smaller than unity if, for example, there is any stray coupling between the input and output guides.

In the cross state, most of the input light (a fraction α_2) will exit from output 4. Therefore, allowing for propagation losses:

$$P_3 \text{ (cross)} = (1-\alpha_2). \gamma . P_1 \tag{20}$$

$$P_4 \text{ (cross)} = \alpha_2 . \gamma P_1 \tag{21}$$

α_2 can be considered as the switch efficiency, and can be much less than unity, depending on the quality of the switch. From equations 18-21, we can define the extinction ratios for the bar and cross states, where the output power is primarily in outputs 3 and 4 respectively.

$$R \text{ (bar)} = P_3 \text{ (cross)}/P_3 \text{ (bar)} = (1 - \alpha_2)/\alpha_1 \tag{22}$$

$$R\ (\text{cross}) = P_4\ (\text{bar})/P_4\ (\text{cross}) = (1-\alpha_1)/\alpha_2 \tag{23}$$

Note: The extinction ratio is often referred to as the cross-talk or on/off ratio in publications.

9.3. Appendix 3: Calculation of signal-to-noise ratio in a partial-tap non-blocking array using X-type switch elements

Consider the M x M integrated optical switch array shown in Fig. 16, where each element consists of a coupler section C, a switch S, and an intersection A (Fig. 18). It is assumed that the coupler in column j taps a fraction T_j of the power in the input guides, where:

$$T_j = 1/(M+1-j) \tag{24}$$

The switch is characterised by two parameters, α_1 and α_2, which were defined in Appendix 2. The intersection, A, is characterised by a parameter α_3, which is the fraction of the input power which is transmitted straight through the intersection. It is assumed that there is no propagation loss in these calculations.

The signal-to-noise ratio (SNR) of the outputs of the array can be determined by calculating the levels of the wanted and unwanted signals. Consider an M x M array, with a signal of power P in each input. In the worst case, the selected input is furthest from the output i.e. $i=M$. The signal P_s at the output of the array (for column $j=1$) is given by:

$$P_s = \frac{P}{M}\left\{\alpha_2 + (1-\alpha_2)(1-\alpha_3)(M-1)\right\}(\alpha_1\alpha_3)^{(M-1)} \tag{25}$$

The total cross-talk signal, P_c, is the sum of the unwanted signals from all of the other inputs:

$$P_c = \frac{P}{M}\left\{(1-\alpha_1) + \alpha_1\,(M-1)(1-\alpha_3)\right\}\sum_{i=1}^{M-1}(\alpha_1\alpha_3)^{(i-1)} \tag{26}$$

Equation 26 can be simplified to give:

$$P_c = \frac{P}{M}\,\frac{\left\{(1-\alpha_1) + \alpha_1\,(M-1)(1-\alpha_3)\right\}\left\{1-(\alpha_1\alpha_3)^{(M-1)}\right\}}{\left\{1-\alpha_1\alpha_3\right\}} \tag{27}$$

The SNR is then given by:

$$\text{SNR} = P_s/P_c = \frac{\left\{\alpha_2 + (1-\alpha_2)(1-\alpha_3)(M-1)\right\}\left\{1-\alpha_1\alpha_3\right\}}{\left\{(1-\alpha_1) + \alpha_1\,(1-\alpha_3)(M-1)\right\}\left\{(\alpha_1\alpha_3)^{(1-M)}-1\right\}} \tag{28}$$

It is possible to reduce the cross-talk level by modifying the switch element (Fig. 20). The coupler has been replaced by a second X-type switch S_2. It is assumed that S_2 is in the off or bar state when the input is not selected. In this case the SNR is given by:

$$\text{SNR} = \frac{1}{M}\,\frac{\left\{\alpha_2 + (1-\alpha_2)(1-\alpha_3)(M-1)\right\}\left\{1-\alpha_1\alpha_3\right\}}{\left\{(1-\alpha_1)^2 + \alpha_1^{\,2}\,(1-\alpha_3)\right\}\left\{(\alpha_1\alpha_3)^{(1-M)}-1\right\}} \tag{29}$$

9.4. Appendix 4: List of symbols

b	The normalised guide refractive index.
d	The electrode separation in an X-type switch.
g	The waveguide separation in a directional coupler.
h	The thickness of the high-index layer of a waveguide.
i	The label of a row in a partial-tap, non-blocking switch array.
j	The label of a column in a partial-tap, non-blocking switch array.
k	The magnitude of a wavevector K in free-space.
k_f	The magnitude of the wavevector K in the waveguide.
m	The mode number of the modes of the waveguide.
n_f, n_c n_s, n_l	The refractive indices of the film, cover, substrate, and loading layers of a waveguide, respectively.
x y z	The orthogonal coordinate system for the waveguide.
A	The intersection of the stripe waveguides in a partial-tap switch element.
C	The coupler in a partial-tap switch element.
D	The interaction length of a directional coupler.
K	The wavevector of the rays in a waveguide.
L	The coupling length of a directional coupler.
M	The number of inputs/outputs of a switch array.
N	The effective refractive index of a guided mode.
P	Optical power.
R	Extinction ratio of a 2-way change-over switch.
S, S_2	An X-type switch.
T_j	The fraction of the input beam switched by a partial-tap switch element.
V	The normalised frequency of a waveguide.
W	The width of a stripe waveguide.

X	Type of switch.
α_1	Straight-through transmission efficiency of a switch.
α_2	Switching efficiency of a switch.
α_3	Straight-through transmission efficiency of a waveguide intersection.
β	The propagation constant of a guided mode.
γ	The propagation loss through a switch.
Δ	The difference in refractive indices of the film and substrate layers.
$\Delta\beta$	The difference in the propagation constants of the two guides in a directional coupler.
θ	The angle of incidence of a ray at the film/cover or film/ substrate interface.
λ	Wavelength in vacuo.
λ_o	The wavelength of peak reflectivity of a corrugated-waveguide filter.
λ_{pm}	The phase matched wavelength of a directional coupler filter.
λ_{tpm}	The phase matched wavelength of a directional coupler filter with an applied tuning voltage.
ω	The period of the grating in a corrugated waveguide filter.

Printed by BBC RESEARCH DEPARTMENT, Kingswood Warren, Tadworth, Surrey, KT20 6NP